Article

Formation of the Yamal Crater in Northern West Siberia: Evidence from Geochemistry

Sergey Vorobyev [1], Andrey Bychkov [1] , Vanda Khilimonyuk [1,*], Sergey Buldovicz [1], Evgeny Ospennikov [1] and Evgeny Chuvilin [2,*]

[1] Department of Geology, Lomonosov Moscow State University (MSU), GSP-1, Moscow 119991, Russia; vsa46@mail.ru (S.V.); andrewbychkov@rambler.ru (A.B.); ser_bul@rambler.ru (S.B.); neogeoman@mail.ru (E.O.)

[2] Skolkovo Institute of Science and Technology (Skoltech), Moscow 121205, Russia

* Correspondence: wandahs@gmail.com (V.K.); e.chuvilin@skoltech.ru (E.C.)

check for updates

Abstract: In the framework of this work, studies on the Yamal crater formed as a result of a cryogenic eruption of a water-gas fluid were carried out. The structure and variations of the composition of the geochemical field along the section of the upper horizons of permafrost are considered on the basis of field work, including the drilling of boreholes near the crater. The obtained regularities of the distribution of chemical elements, and gases between the mineral component of the soil and meltwater, suggest that permafrost at the site of the funnel are the remains of a sub-lake paleo-talik, from which mineralized water and gases were expulsed into the yet unfrozen reservoir that previously existed at this place. The component composition of gases suggests that they are products of biochemical processes similar to those that occur in modern peatlands. The $\delta^{13}C$ value for methane extracted from the sediments of the near-contact zone of the Yamal crater was found to be $-76‰$. The predominance of high molecular weight normal alkanes in frozen bitumen indicates that the original organic substrate which was buried contained remains of higher vegetation. The Yamal funnel was formed by the sediment's "explosion" while the water-gas fluid was released. The volume of the ejected sediment amounted to about 220 thousand m^3.

Keywords: Yamal Peninsula; Yamal crater; gases in permafrost; geochemical studies; talik; gas generation; methane; carbon dioxide; freezing; gas outburst

1. Introduction

A cylindrical crater, at least 50 m deep and 20–25 m in diameter (Figure 1), was discovered in June 2014 in the Yamal Peninsula 30 km south of the Bovanenkovo oil-gas-condensate field.

The crater has been described in detail in previous publications [1–5]. It formed in the place of a large pingo produced by long-term lateral back freezing of a paleo-talik beneath a past thaw lake on the bottom of a thermokarst depression [5]. The authors [5] have examined in sufficient detail the hypothesis of the formation of a large lake talik, as well as its long-term freezing, based on mathematical modeling of heat transfer in rock strata. In the same place [5], the explosion conditions of the formed heaving mound with the formation of a crater are considered and the stages of this process are described. The existence of thick (over 100 m) or through taliks beneath large drained lake basins of the North of Western Siberia has been confirmed by modern geophysical studies [6].

Figure 1. A fragment of a satellite image of the Earth's surface within the Yamal Peninsula indicating the location of the crater (**left**) and a view of the explosion crater from a helicopter (**right**). 1, 2, 3 contours: crater vents, explosion funnels, and parapet of parapet, respectively. Named points mark wells and their numbers.

Most likely is that the crater originated from a sudden outburst of pressurized gas upon collapse of its subsurface reservoir, judging by the absence of visible signatures that would indicate a thermal effect on the rocks. Abrupt decompression led to avalanche-like degassing and eruption of the unfrozen gas reservoir. The gas release was possibly triggered by instantaneous crystallization of supercooled gas-saturated water or by dissociation of sub-pingo gas hydrates.

In June 2015, a team from Moscow University (Department of Geology) undertook a field trip to study the crater and its vicinities by geocryological, geochemical, geophysical, and radiometric methods, with the support of the Innopraktika and NOVATEK companies [5]. The cryostratigraphy and composition of permafrost in the area were studied along a profile that traversed the crater in the North East direction (Figure 1), with core sampling obtained from seven 10 to 17 m deep boreholes.

According to the core data, the section consists of marine, lacustrine, fluvial, and slope wash clay, clay silt, and silt that enclose poorly degraded peat and remnants of shrub roots and twigs.

2. Methods

The boreholes were sampled every ~1 m and the retrieved core was cleaned from material that contacted the hole walls. Sampling, storage, and analysis were performed in full compliance with the guidelines governing the order of geological and geochemical work in the search and exploration of hydrocarbon deposits. The time from selection to receipt of analytical data did not exceed 10 days. The gas component of permafrost was studied in 10 cm long core samples from specified depths placed in 0.5 L glass vessels, which were then filled with a saturated NaCl solution to a volume measured to an accuracy of 0.5 mL, and some salt was added to compensate dilution by meltwater. The vessels were sealed under metal lids covered with plastic, turned upside down, and transported to a laboratory. The selected samples were represented by loamy and clayey soils with ironing spots and inclusions of individual lenses of plant detritus of the Middle-Late Pleistocene (m III_{2-3}) and Holocene deposits [7]. At the same time, samples of surrounding rocks were collected in plastic bags for chemical analyses. The species and contents of gases were analyzed in 118 and 103 samples, respectively.

The contents of methane and carbon dioxide were measured in drill holes twice a day during the whole field campaign by a Seitron gas analyzer with a range of 1 to 10,000 ppm for CH_4 and an optical interferometer with a range of 0.1 to 6 vol.% for CO_2. The gas flux from the boreholes was estimated by air expulsion from a vessel of known volume (5 L) using a gas analyzer which was placed inside.

In the laboratory, gas was retrieved from sealed samples by thermal-vacuum degassing (the TVD method). During thermal vacuum degassing in a vacuum, each sample heated to 65–75 °C. The evaluated gas volume and the dry rock weight were used to calculate gas and ice contents in permafrost. Total core gas content varied from 17 to 233 mL/L depending on the location of the sampling points with respect to the crater walls and the ice content. The average gas content of samples was 99.5 mL/L. Gas species were identified by gas chromatography. All samples were analyzed for inorganic (He, H, CO_2, O_2, and N_2) and organic (CH_4 and its 40 homologs) gases.

It was impossible to constrain the gas volume per unit weight of rocks because of ice content variations; the gas contents were recalculated per unit volume of undisturbed permafrost. Table 1 lists the maximum and minimum contents of main gas components in permafrost around the crater.

Table 1. Contents of intrapermafrost gases around the Yamal crater.

Parameter	He	CO_2	H_2	O_2	N_2	CH_4	C_2H_6
	Relative to Total Gas, Vol.%						
C_{max}	1.3×10^{-3}	40.3	13.3	19.81	89.1	13.2	2.5×10^{-3}
C_{min}	4.8×10^{-3}	0.48	0.00014	0.03	45.4	7.1×10^{-4}	8.5×10^{-6}
	Relative to Permafrost, Vol.%						
C_{max}	1.7×10^{-4}	7.8	1.18	1.84	11.6	1.2	2.1×10^{-4}
C_{min}	4.2×10^{-5}	0.04	1.8×10^{-5}	0.0012	1.79	2.6×10^{-4}	4.6×10^{-6}

Major-element contents in rock samples were analyzed using the X-ray fluorescence (XRF) method, and trace elements were determined by mass spectrometry with inductively coupled plasma. (ICP-MS). Processing and mapping of geochemical data was performed by means of GIS "Gold-Geochemist", developed at the Department of Geochemistry of Lomonosov Moscow State University.

3. Results

3.1. Chemical Aureoles around the Yamal Crater

3.1.1. Lithochemical Aureoles

The rocks within the sampled section were found to be compositionally uniform and the patterns of major and trace elements were observed to have no spatial relation to the crater wall contours. According to cluster analysis, the samples fall into two groups located south and north of the crater (Figure 2).

The North group includes deeper samples from the northern and central parts of the profile where ice contents in permafrost exceeds 75%, and the South group includes samples from the southern profile part and shallower samples from the north, all of which have lower ice contents.

The contents of major and trace elements in the two groups of samples were found to have no statistical difference, but the composition difference shows up in deviations of group average element contents ($\overline{C_{ij}}$) from the average values over the whole profile ($\overline{C_i}$). This difference was normalized to the standard deviation s_i in order to obtain dimensionless values (Figure 3).
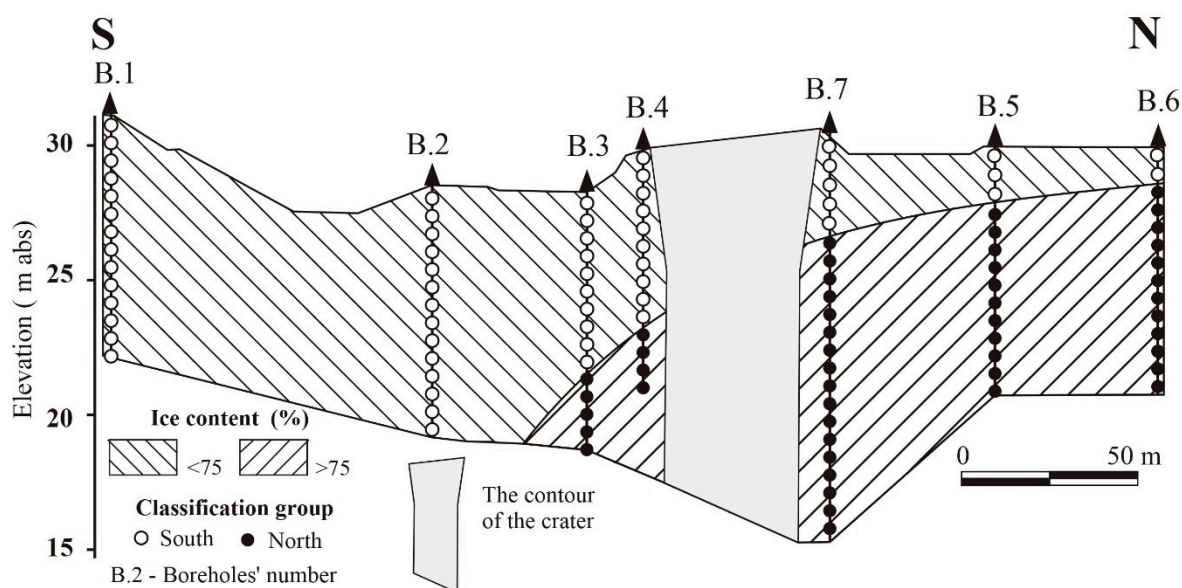
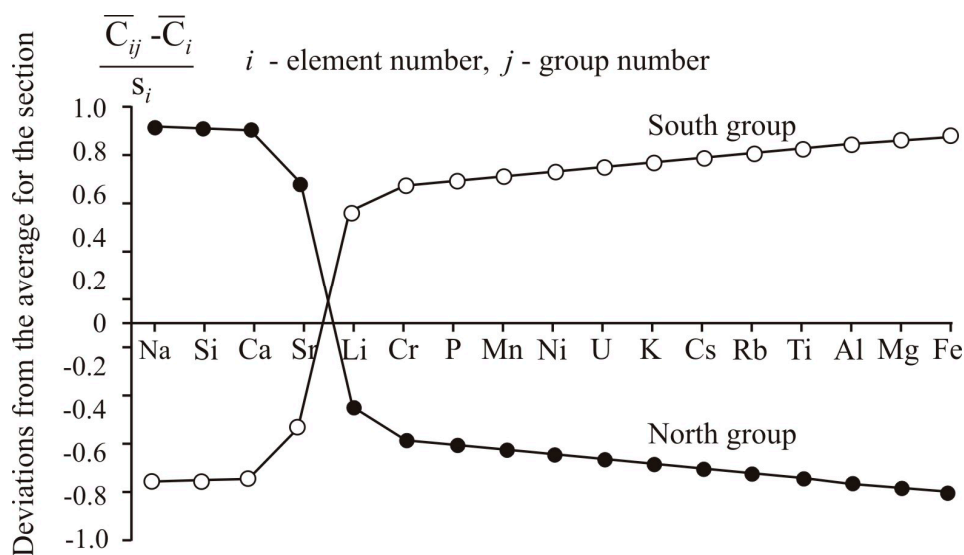**Figure 2.** Classification of permafrost samples from around the Yamal crater.

Figure 3. Major- and trace-element contents in samples from the South and North groups' deviation from the profile average. C_i and S_i indicate the average element content and standard deviation along the section. C_{ij} indicates the average content of the elements in the classification group.

The curves in Figure 3 show that the ice-rich samples of the North group contain more Si, Ca, and Na than those of the South group but less Al, Mg, Fe, and K (which are common to clay minerals). The mirror symmetry of the curves about the profile average line indicates that the elements removed during freezing from the ice-rich rocks of the North group were redeposited in those of the South group. Since the total element contents always approaches 100%, the loss of mobile compounds leads to a relative increase of less mobile ones, which explains the higher concentrations of Si, Ca, and Na in the North group samples. The distribution of elements between the mineral phase of frozen rocks and ice was most contrasted for calcium within the studied section.

The zones of high and low contents of Ca in the mineral and ice components of the samples are located in different parts of the profile (Figure 4), which is evidence of Ca partitioning between the water and mineral phases when the paleo-talik was freezing back. Unfrozen water contains elements released from ice-rich rocks, i.e., some water-active mobile compounds became leached from minerals in permafrost, leaving quartz with minor amounts of plagioclase and clay minerals.
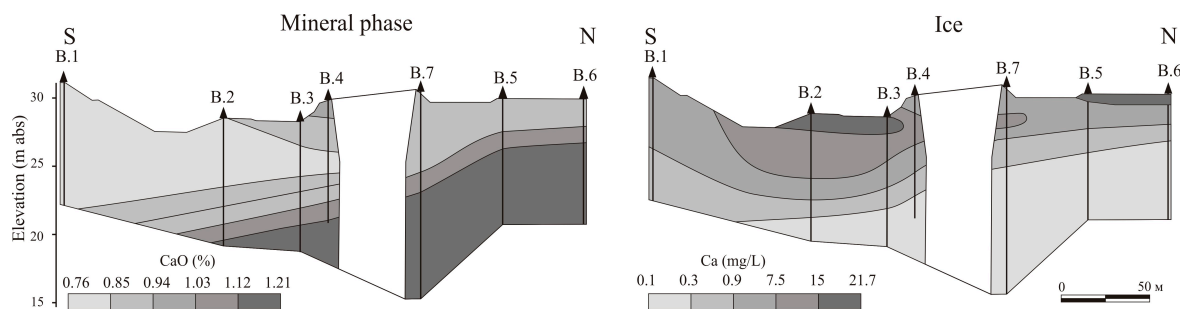
Figure 4. Distribution of Ca in mineral and ice phases of rocks around the Yamal crater.

The partitioning of elements between the water and mineral phases of the samples provides evidence that ice-rich rocks (>75% ice contents) belong to the paleo-talik. Gases and saline water were expulsed from the talik into the yet unfrozen reservoir beneath the pingo, and the eruption of fluid (water and gas) increased the salinity of rocks around the crater. The salinity increase left an imprint in the composition of water which drained the rocks and acquired salinity markedly above the local background, despite dilution with rainfalls and melting snow after the eruption. An increase in surface water salinity in puddles near the crater was also recorded. The volumes of unfrozen water and rock can be preliminarily estimated from the mass balance of elements in the water and mineral phases. According to estimates, the water/rock ratio for clastic sediments in the paleo-talik is approximately 1000 to 10,000.

3.1.2. Gas Aureoles

The intrapermafrost gas phase in the crater area comprises mainly N_2, CO_2, O_2, H, and CH_4. The maximum contents of CO_2, H_2, and CH_4 are orders of magnitude higher than the recorded background. Oxygen varies from atmospheric values to hundredths of a percent. The contents of gases and other elements in the permafrost around the crater correlate with the ice contents (Table 2).

Table 2. Contents of gases in the permafrost around the crater.

Group	Ice Content (%)	Characteristic	Gas Content (%)					
			N_2	CO_2	O_2	H_2	CH_4	He
North	81.1	Average	78.6	10.8	3.1	2.7	2.3	0.00041
		C_{min}	55.1	3.5	0.03	62.3	27.9	0.00008
		C_{max}	89.1	21.8	7.8	13.1	13.8	0.00015
South	53.1	Average	64.5	18.4	7.9	0.37	2.7	0.00054
		C_{min}	45.4	0.5	0.5	0.2	4.7	0.00009
		C_{max}	87.7	40.3	19.8	3.3	10.4	0.00012
Background		Average	77.1	9.2	7.2	0.0008	0.0006	0.0003

The contents of carbon dioxide and oxygen in the samples from the northern part of the profile are on average twice as low as those from the south. Hydrogen is almost ten times higher, while methane does not differ much across the two profile parts; helium is about that of the background level. This distribution is inconsistent with CO_2, H_2, and CH_4 inputs from greater depths along faults or fractures that crosscut the pingo.

Gases can be observed to have more intricate vertical patterns (Figure 5) than major and trace elements. The near-surface zone of high gas saturation reaches a depth of 7 m. The distribution of gas contents in rocks apparently corresponds to that prior to the eruption event: it is highest between 3 and 5 m below the surface and decreases smoothly to the background values above and below this range. Carbon dioxide shows a distribution similar to that of gas saturation and thus may be a key component of the gas mixture expulsed into the unfrozen zone beneath the pingo when the talik was freezing.
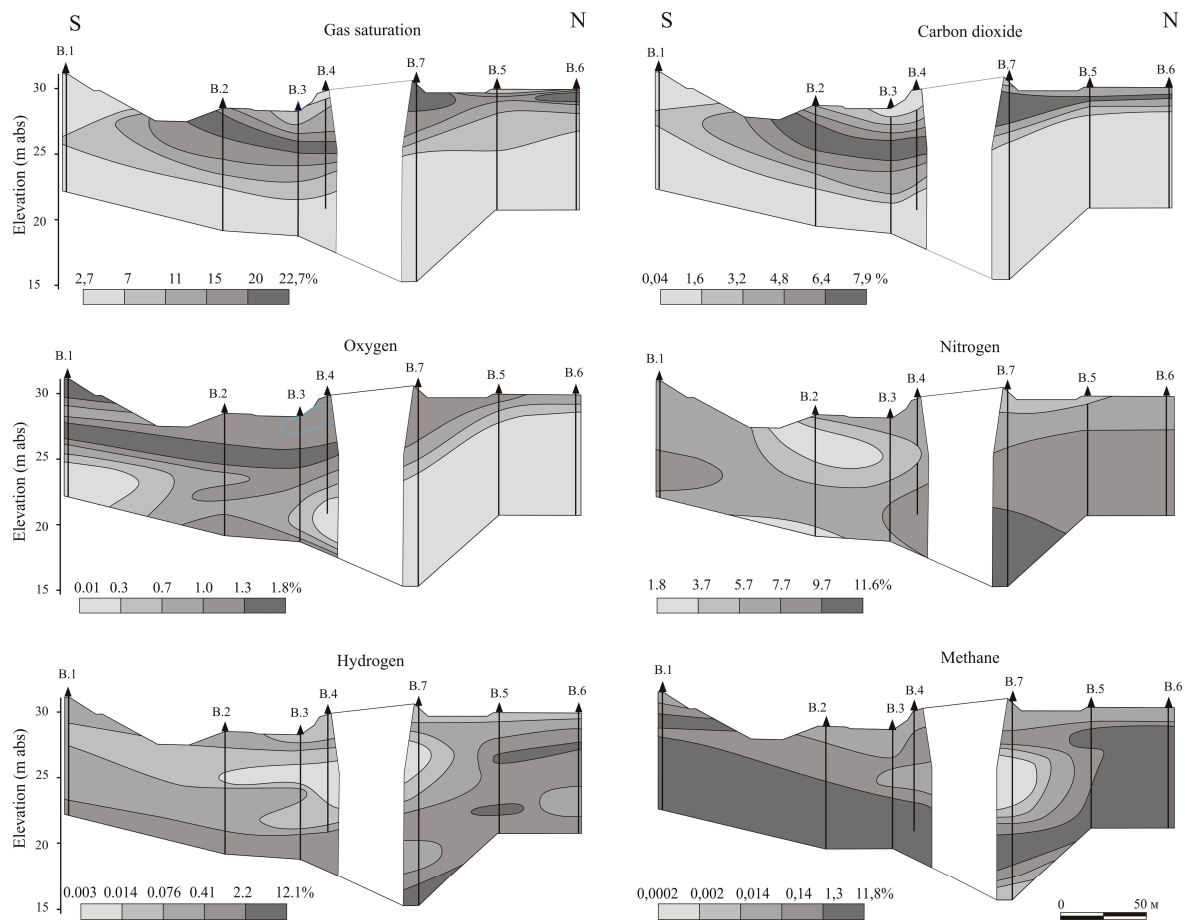
Figure 5. Vertical patterns of gas saturation and contents of CO_2, O_2, N_2, H, and CH_4 in rocks around the crater.

Oxygen is significantly below the atmospheric value and is less regularly distributed with depth compared to other gases, which may be due to permeability variations in the section. Zones of low O_2 are located in ice-rich rocks north of the crater. H and CH_4 have similar patterns with a zone of highest values variable in thickness but running continuously over the lower part of the section and a zone of low contents encircling the crater 4–5 m below its top.

The original distribution of gases in the area remains unknown. It formed as the talik was freezing back and the gases it stored were expulsed by the freezing front, together with saline water, into the yet unfrozen sub-pingo zone. That zone made up a core with gas- and water-filled porosity corresponding to a zone of low H and CH_4 in the gas field; large amounts of these highly mobile volatiles were released from wall rocks into the atmosphere during the cryovolcanic event.

Measurements of gas flow at the borehole head show that it migrated into the near-surface air for 2–3 days at variable rates. The flow rate was highest from boreholes in the southern part of the profile where the rocks have lower ice contents and reached 5×10^{-4} L·s^{-1}·m^{-2} per unit surface of the borehole wall at the end of drilling. The content of methane emanating from drill holes was at least twice as high as the average in the core samples, e.g., methane in the free gas phase from borehole (B.4) was in the range 0.48% to 0.67%, but pore methane was only 0.16% on average. This dramatic difference indicates that gas can migrate through active voids in permafrost and thus penetrate into boreholes from remote parts of the section.

The correlation relationships between the components of subsurface gases (Figure 6) reveal two groups with opposite trends: (1) CO_2, O_2, and He and (2) CH_4 and H. The gases of group 1 are in

positive correlation with gas saturation, which indicates that they originated from the same source, i.e., the freezing sub-lake paleo-talik.
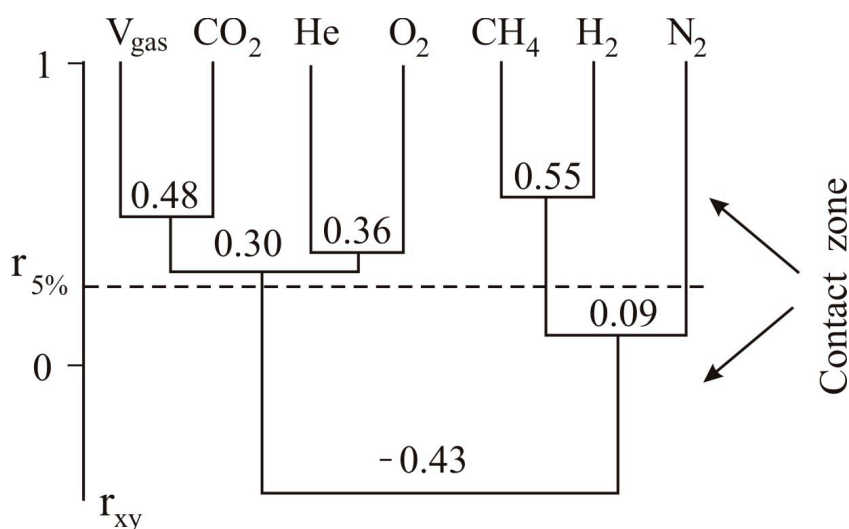

Figure 6. Correlations between the contents of subsurface gases around the Yamal crater. r5% is the critical value of the correlation coefficient for a 5% significance level.

The gases in the crater walls are marked by a positive correlation between CO_2 and O_2 (Table 1), unlike those above faults and mineral deposits or oil and gas fields, where they are in negative correlation. The correlation is negative in the latter case because CO_2 is either a product of oxidation reactions or a component of deep-seated gases which release near the surface and thus reduce the content of atmospheric gases in the pore space. The positive correlation between CO_2 and O_2 is evidence of their joint input into the crater from the freezing talik.

Carbon dioxide and nitrogen are the principal components of the intrapermafrost gas phase in the crater area. They reach a total content of 71% to 99% and make up a closed two-component system where an increase of one component corresponds to a decrease of the other. Nitrogen is an inert gas which does not participate in reactions and its content in the rocks fully depends on that of CO_2; the two are related as $N_2 = 87.6 - CO_2$. The free term of this relationship corresponds to the initial concentration of nitrogen in the subsurface gas phase, which is fully consistent with the results of gas surveys from different years in northern Russia. Inputs of gas from the freezing talik locally make the content of N_2 almost twice as low. The strong positive correlation of CO_2 with gas saturation and the negative correlation with nitrogen indicates that CO_2 was the principal subsurface gas component in the freezing talik and that its pattern controlled the contents of other gases in rocks around the crater.

3.2. Origin of Gases in the Yamal Crater Area

The Yamal crater is located 60 km from the Bovanenkovo gas field and it is pertinent to assess their possible relationship. The gas phase in the reservoir rocks of the Bovanenkovo field contains 98.9% methane and 0.22% ethane, with only minor N_2 and CO_2, according to unpublished data collected by the Department of Geology and Geochemistry of Fuel Deposits at Moscow University. The carbon isotope composition of the Bovanenkovo methane is about −39.9‰ $\delta^{13}C$. The rocks in the crater walls store much more CO_2, N_2, and H_2 than those in the gas field. The weighting of the isotopic composition of methane carbon is $\delta^{13}C = -76$‰. This difference disproves the hypothesis that the gas that exploded in the Yamal crater could have come from the Bovanenkovo reservoirs.

The gas composition in the samples we analyzed corresponds to that resulting from biochemical processes in paludal environments. The carbon isotope composition of marsh methane, more depleted than that of methane from gas and gas-condensate reservoirs, is controlled by the composition of degrading organic matter and biochemical reactions of methane formation.

The more negative $\delta^{13}C$ values of CH_4 may be due to its formation by CO_2 reduction, further oxidation of CH_4 by methanotrophic bacteria, and fermentation of methylated organic compounds without subsequent oxidation. Methane obtained by bacterially-mediated reduction of CO_2 has $\delta^{13}C$ values reaching −110‰, while the fermentation of methylated dead plant material gives a $\delta^{13}C$ range of −50‰ [8]. In Siberian peatlands, the range for biochemical methane is −71 to −77‰ $\delta^{13}C$ [9], which includes the $\delta^{13}C$ value of −76‰ in methane released from the Yamal crater.

The origin of hydrocarbon gases at different core depths around the crater was inferred from bitumen contents distributed evenly along the section, with the relative contents of alkane species given in histograms of Figure 7. Judging from the obvious predominance of high-molecular alkanes ($C_{19}H_{40}$ and higher), buried plant remnants are the primary organic substrate present. Lipids of higher plants are rich in even-chain fatty acids and tricosane produced by decarboxylation of saturated fatty lignoceric acid, a typical high-molecular organic component of higher plants. The pristan/fitan ratio of 0.68 (<1) indicates reduced euxinic conditions of diagenesis [10].
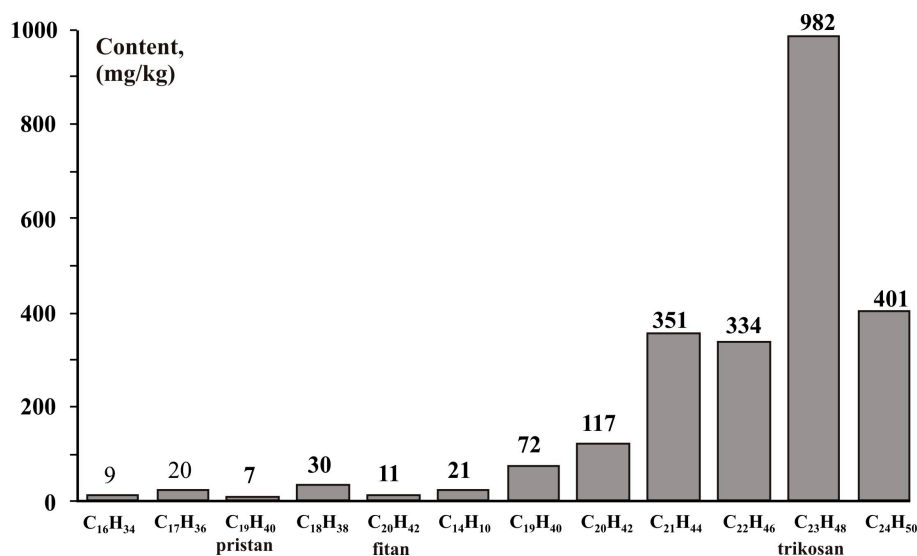
Figure 7. Contents of alkanes (ppm) in the cored section.

Biochemical transformation of organic matter is accompanied by rapid gas generation. Methane, a major component of the gas phase in degrading buried matter, is produced by anaerobic bacteria (mainly the *Methanobacterium, Methanococus,* and *Methanosarcina* genera) from CO_2, H_2, acetate, and fatty alcohols resulting from cellulose fermentation by other bacterial species. In euxinic environments, the reactions are [11]

$$C_6H_{12}O_6 + 6H_2O = 6CO_2 + 12H_2$$

$$CO_2 + 4H_2 \rightarrow CH_4 + 2H_2O$$
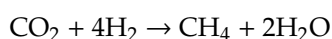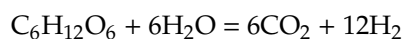
Thus, each cellulose molecule decomposing during biochemical transformation of plant organic matter releases eight molecules of hydrogen while producing one CH_4 molecule. The carbon isotope composition of the reaction products is −75‰ to −80‰ $\delta^{13}C$ [9].

Marsh gases also store quite large amounts of hydrogen, occasionally making up up to 2% of the total gas volume [12]. We compared relative percentages of gases isolated from the lake and marsh water in the depression that accommodates the crater at its southern edge and found about ten times higher contents of dissolved hydrogen and methane in marsh water compared to that in the lake: $H_2 = 0.0081$ and $CH_4 = 0.46$ against $H_2 = 0.00016$ and $CH_4 = 0.039$, respectively. Note that in both cases the samples were from water that contacted the atmosphere, which favors the escape of poorly soluble gases such as hydrogen and methane.

3.3. Volume of Exploded Gas

The volume of gas that migrated into the unfrozen zone remaining beneath the pingo cannot be reliably constrained from gas contents in the frozen part of the paleo-talik because the original talik underwent a complex evolution and diverse physical processes in the course of long-term lateral freezing. Specifically, it is impossible to estimate the loss of gas by cryogenic concentration at an early stage when the primary lakes still existed.

Nevertheless, the volume of gas that exploded and caused the crater formation can be estimated within the first approximation proceeding from the volume of the frozen talik part and its remnant gas saturation. According to estimates of gas redistribution during freezing of methane-saturated sand, up to 75 vol.% of gas can be expulsed into the unfrozen zone while 25 vol.% can remain in the rock [13,14]. In our case, the remnant gas in the sediments, which have fine grain sizes, may occupy 50 vol.%.

We estimate that pingo formation involved 220,000 m^3 of frozen rock, which is consistent with the volume of ground ice recorded by geophysical surveys of the surroundings of the crater.

Laboratory studies of rock physics in the core samples indicate the presence of free gas in the pore space free from ice or liquid water in rocks between the boreholes, as well as gas bubbles in ice inclusions. Gas fills 12.5 vol.% of the pore space in permafrost on average, while the average pore gas pressure is 2 bars. With these values, the gas volume in the frozen part of the paleo-talik at the time when it became closed under normal conditions can be estimated to have exceeded 50,000 m^3. About the same amount of gas apparently moved into the unfrozen zone beneath the pingo, given that 50% of the total gas content remained in the frozen part upon the talik freezing. In fact, this volume may have been much greater initially because the rocks around the crater lost much gas during post-eruption degassing, which was observed in the boreholes.

4. Conclusions

The trends of gas distribution in permafrost samples from boreholes drilled around the Yamal crater discussed in this work show that the processes responsible for generation of the exploded gas are largely similar to those in modern paludal environments. Partitioning of some major and trace elements between the mineral and ice components indicates that deeper ice-rich rocks in the northern part of the profile may belong to the sublake paleo-talik. Gas from the talik was expulsed by the freezing front into a yet unfrozen zone of sediments beneath the pingo and was made part of a water and gas fluid.

Judging by the compositions of the mineral and gas components of permafrost, the crater is located at the edge of the freezing talik. The elements had been partitioning between the liquid and solid phases for a few thousand years while the talik was freezing, and biogenic reactions transformed organic matter. As a result, high-molecular compounds of peat and mud communities converted to fulvic and humic acids, while bacteria metabolized organic matter and formed CO_2, CH_4, and H_2, the main gas species found in ice-rich sediments within the frozen paleo-talik.

The results obtained for the upper part of the section for drilled boreholes confirm the presence of cryogenic gas separation during the freezing of a closed thawed rock mass. The gas composition transformations have their own specifics for different depths of the section. Thus, according to estimates of the internal pressure in the talik before the explosion, favorable conditions are created in the lower part of the talik for the formation of carbon dioxide gas hydrates [5].

Author Contributions: Supervision, V.K.; conceptualization and methodology, S.V. and A.B.; field work, V.K., E.O., S.V., and A.B.; laboratory research and analysis, S.B., V.K., S.V., A.B.; E.O., and E.C.; writing and editing, S.V., A.B., V.K., and E.C.

References

1.　Leibman, M.O.; Plekhanov, A.V. The Yamal gas burst crater: Results of a preliminary study. *Kholod'OK* **2014**, *12*, 9–15. (In Russian)

2.　Bogoiavlenskiy, V.I.; Mazharov, A.V.; Pushkarev, V.A.; Bogoyavlenskiy, I.V. Gas bursts in permafrost of the Yamal Peninsula: Preliminary field data of 8 July 2015. *Bureniye i neft.* **2015**, *7*, 8–13. (In Russian)

3.　Kizyakov, A.I.; Sonyushkin, A.V.; Leibman, M.O.; Zimin, M.V. Geomorphological conditions of the gas-emission crater and its dynamics in Central Yamal. *Earth's Cryosphere* **2015**, *XIX*, 13–22.

4.　Olenchenko, V.V.; Sinitsky, A.I.; Antonov, E.Y.; Eltsov, I.N.; Kushnarenko, O.N.; Plotnikov, A.E.; Potapov, V.V.; Epov, M.I. Results of geophysical surveys of the area of "Yamal crater", the new geological structure. *Earth's Cryosphere* **2015**, *XIX*, 84–95. (In Russian)

5.　Buldovicz, S.N.; Khilimonyuk, V.Z.; Bychkov, A.Y.; Ospennikov, E.N.; Vorobyev, S.A.; Gunar, A.Y.; Gorshkov, E.I.; Chuvilin, E.M.; Cherbunina, M.Y.; Kotov, P.I.; et al. Cryovolcanism on the Earth: Origin of a spectacular crater in the Yamal Peninsula (Russia). *Sci. Rep.* **2018**, *8*, 13534. [CrossRef] [PubMed]

6.　Shein, A.N.; Olenchenko, V.V.; Kamnev, Y.K.; Sinitsky, A.I. The structure of the freezing lake talik at the hospit al in Parisento (Gydan Peninsula) according to the data of electrotomography. In Proceedings of the Interexpo Geo-Siberia, XV International Scientific Congress, Novosibirsk, Russia, 24–26 April 2019; pp. 103–110. (In Russian).

7.　Khilimonyuk, V.Z.; Ospennikov, E.N.; Buldovich, S.N.; Gunar, A.Y.; Gorshkov, E.I. Geocryological conditions of the territory of the Yamal crater. In Proceedings of the 5nd Russian Conference on Geocryology, Lomonosov Moscow State University, Moscow, Russia, 14–17 June 2016; pp. 245–255. (In Russian).

8.　Whiticar, M.J. Carbon and hydrogen isotope systematics of bacterial formation and oxidation of methane. *Chem. Geol.* **1999**, *161*, 291–314. [CrossRef]

9.　Glagolev, M.V.; Smagin, A.V. Quantification of methane emission in paludal environments, from profile to regional scale. *Dokl. po Ekol. Pochvovedeniyu* **2006**, *7*, 75–107. (In Russian)

10.　Tissot, B.P.; Welte, D.H. (Eds.) *Petroleum Formation and Occurrence*; Springer: Berlin/Heidelberg, Germany, 1978; p. 538. ISBN 978-3-642-87813-8.

11.　Bazhenova, O.K.; Burlin, Y.K.; Sokolov, B.A.; Khain, V.E. *Petroleum Geology and Geochemistry*; Sokolov, B.A., Ed.; Moscow University Press: Moscow, Russia, 2000; p. 384. ISBN 5-211-04888-1. (In Russian)

12.　Lukiyanova, T.S.; Mansurov, G.N. Marsh gases as a natural cause of spontaneous ignition in paludal environments. *Vestn. Mosc. State Reg. Univ.* **2012**, *2*, 161–167. (In Russian)

13.　Yakushev, V.S.; Chuvilin, E.M. Natural gas and gas hydrate accumulations within permafrost in Russia. *Cold Reg. Sci. Technol.* **2000**, *31*, 189–197. [CrossRef]

14.　Kraev, G.; Schulze, E.-D.; Kholodov, A.; Chuvilin, E.; Rivkina, E. Cryogenic displacement and accumulation of biogenic methane in frozen soils. *Atmosphere* **2017**, *8*, 105. [CrossRef]